Metallurgy and materials
Metalurgia e materiais

Potassium recovery from Brazilian glauconitic siltstone by hydrothermal treatments

Frederico Amorim Safatle[1,2]
   https://orcid.org/0000-0003-4588-5458
Kátia Dionísio de Oliveira[1,3]
   https://orcid.org/0000-0002-6267-5383
Cícero Naves de Ávila Neto[1,4]
   https://orcid.org/0000-0002-5835-6670

[1]Universidade Federal de Uberlândia – UFU,
Faculdade de Engenharia Química,
Uberlândia – Minas Gerais – Brasil.

E-mails: [2]fredsafatle@gmail.com,
[3]katiadionisiolveira@gmail.com, [4]avilaneto@ufu.br

Abstract

Silicate rock Verdete, collected in the central region of Minas Gerais state (Brazil) and composed mostly of micas (glauconite and muscovite) and tectosilicates (K-feldspar and quartz), was hydrothermally treated with several reactants in order to release and recover potassium. The hydrothermal products were characterized by flame photometry, XRD, XRF, SEM and EDS. Treatment with sulfuric acid was effective to break the crystal lattice of micas before 1 h of reaction and recovered 24% of potassium in the form of sulfates. The K-feldspar appears to have remained intact during the process. Treatment with a $Ca(OH)_2$ (86 wt.%) - $CaCO_3$ (14 wt.%) mixture did not consume the micas, but K-feldspar was gradually consumed over the 24 h reaction period. The K recovery was probably due to a concurrent hydrolytic framework dissolution of K-feldspar mediated by OH^- ions and by the exchange of K^+ with Ca^{2+}. The K-bearing species are carbonaceous materials with variable K^+/Ca^{2+} ratios, such as $K_2Ca(CO_3)_2$.

Keywords: hydrothermal treatment; potassium recovery; muscovite; glauconite; K-feldspar.

1. Introduction

The main sources of potassium for use as fertilizer are underground deposits of soluble minerals (denominated potash), such as silvinite and carnalite; and pickles, such as those situated in inland seas and salt flats. According to statistics compiled by the U.S. Geological Survey (2018), potassium salt reserves occur predominantly in the northern hemisphere, in countries such as Canada, Russia and Belarus, which together hold the vast majority of world`s potash. Brazil is in a delicate situation, because although it is one of the countries that most demands potassium in the world, its domestic production, in the exclusive form of KCl, produced only in the Taquari-Vassouras complex (Sergipe state), represents less than 10% of apparent domestic consumption (Teixeira *et al.*, 2012).

Silicate rocks composed of feldspars, muscovite, glauconite, phlogopite, biotite, feldspathoids, zeolites and other minerals are alternatives to potassium salts (Martins *et al.*, 2008). Brazilian silicate rock Verdete is an example. Verdete is a denomination given to sedimentary rocks associated with the Serra da Saudade formation (Minas Gerais state), a deposition whose origin may be related to a rapid generalized marine

transgression, in which sediments rich in clay minerals would have been precursors for diagenetic substitution with K^+ from sea water, in the Neoproterozoic Era (Moreira *et al.*, 2016). The rock consists essentially of a mixture of micas (mostly glauconite and muscovite) and tectosilicates (quartz and K-feldspar), with K_2O equivalent content between 7 and 14% (Piza *et al.*, 2011; Moreira *et al.*, 2016; Santos *et al.*, 2016).

Publications dealing with the acidic dissolution of silicate rocks date back to the early 20th century (Cushman and Hubbard, 1908). Varadachari (1992) showed that potassium can be recovered from biotite through concentrated acidic solutions. The behavior of biotite in acidic solutions is different from the behavior of muscovite, which is very difficult to solubilize except by reaction with phosphoric acid. Although biotite could also be solubilized via reaction with phosphoric acid, the immediate solubility of the mineral in hydrochloric acid (Varadachari, 1997) and sulfuric acid provided more viable alternatives.

Mineral silicates can also be dissolved via hydrothermal routes. Ciceri *et al.* (2017) studied the dissolution of syenite, obtained in Triunfo batholith, located in

Pernambuco state (Brazil). The syenite rock, composed mainly of K-feldspar, was mixed with slaked lime [$Ca(OH)_2$] and placed to react at 473 K for 5 h within hydrothermal reactors. The authors suggested that the mechanism for increasing K content is the hydrothermal alteration of K-feldspar, i.e., the hydrolytic dissolution of the feldspathic structure coupled with exchange of K^+ with Ca^{2+}. Wang *et al.* (2018) recovered potassium from K-feldspar using a hydrothermal methodology with NaOH and $NaNO_3$ as reactants. Similar to Ciceri *et al.* (2017), the potassium recovery mechanism was proposed as an ion exchange step between Na^+ and K^+.

Since Verdete is a mixture of micas and tectosilicates, the performance of the hydrothermal methodology in breaking down the crystalline structures of such minerals is a challenge, whether through the use of sulfuric acid or slaked lime. The objective of this research is to demonstrate the efficiency of the hydrothermal methodology in breaking down the crystalline structures of Verdete minerals (mainly micas, K-feldspar and quartz) in the presence of sulfuric acid or slaked lime, in order to release and recover potassium.

2. Materials and methods

2.1 Sample preparation

Samples of Verdete were collected randomly from rock outcrops in three different sites of the central region of Minas Gerais state (Brazil), inside the municipalities of Cedro do Abaeté and Quartel Geral, at the following UTM coordinates (zone 23 K south): Sample 1 - 7865844/422460; Sample 2 - 7869386/419306; Sample 3 - 7884678/426568. Samples were comminuted twice in a hammer mill and classified (with Tyler sieves) into five discrete size ranges: +35# (500 µm), +60# (250 µm), +100# (149 µm), +200# (74 µm) and -200# (74 µm).

2.2 Hydrothermal treatments

Several reactions were conducted in a set of stainless-steel autoclaves internally coated with Teflon. The autoclaves were placed in a furnace at 463 K, where they remained for a scheduled time. Reactions were carried out with mixtures of Verdete with $CaCl_2$, $MgCl_2$, H_2SO_4 and calcined $CaCO_3$. Reactions with H_2SO_4 and $CaCO_3$ were performed in triplicate, obtaining the mean and standard deviation of each point, while reactions with other reagents were performed only once. The Mg- and Ca-based salts [$MgCl_2·6H_2O$ (Synth, 99%) and $CaCl_2·2H_2O$ (Synth, 99%)] were previously oven dried at 423 K for 48 h. After drying, the resulting products contained 36.1% $MgCl_2$ and 74.83% $CaCl_2$, respectively, the remainder being water. $CaCO_3$ (Cinética Química, 99%) was previously calcined according to the procedure described in the Supplemental Material. Accordingly, the resulting calcined product was composed of 14% $CaCO_3$ and 86% $Ca(OH)_2$ (in mass).

The feed composition of each series of reactions is shown in Table 1. The water to Verdete ratio ($R_{W/V}$) is defined as the mass of water divided by the mass of Verdete. The reactant to Verdete ratio ($R_{R/V}$) is the mass of reactant divided by the mass of Verdete. In the case of series 5 and 6, $R_{R/V}$ is defined as the mass of Verdete divided by the masses of $CaCO_3$ and $Ca(OH)_2$. The concentrations of reactants in each reaction series are: $C_{CaCl2} = 4.1$ mol L^{-1}; $C_{MgCl2} = 1.4$ mol L^{-1}; $C_{H2SO4} = 5$ mol L^{-1}; $C_{Ca(OH)2} = 2.04 \times 10^{-2}$ mol L^{-1}. In the case of $Ca(OH)_2$, as the solubility in water at 298,15 K is low, the value is the same for both RR/V ratios. More information about the feed masses can be obtained in the Supplemental Material.

Table 1 - Feed composition of each series of reactions.

Series	Mass (g)							$R_{W/V}$ [a]	$R_{R/V}$ [b]
	Verdete	H_2O	$CaCl_2$	$MgCl_2$	H_2SO_4	$Ca(OH)_2$	$CaCO_3$		
1	8.5	17	-	-	-	-	-	2.0	-
2	8.5	13.7	13.2	-	-	-	-	1.6	1.6
3	4.7	8.7	-	13.0	-	-	-	1.8	2.8
4	8.5	10.2	-	-	6.8	-	-	1.2	0.8
5	8.5	17	-	-	-	2.61	0.42	2.0	0.4 [c]
6	8.5	17	-	-	-	4.75	0.77	2.0	0.7 [c]

[a] The water to Verdete ratio ($R_{W/V}$) is defined as the mass of water divided by the mass of Verdete.

[b] The reactant to Verdete ratio ($R_{R/V}$) is the mass of reactant divided by the mass of Verdete.

[c] Mass of Verdete divided by the masses of $CaCO_3$ and $Ca(OH)_2$.

The hydrothermal products, composed of a solid fraction and a liquid fraction, were mixed and oven dried at 343 K for 24 h. The dried products were then subjected to flame photometry and X-ray diffraction (XRD) analyzes, as detailed below. Specifically the hydrothermal products obtained after the 10-hour reaction time of series 4 and 6 (see Table 1) were vacuum filtered in order to separate water-soluble and insoluble components. Both fractions (filtered and retained) were oven dried at 343 K for 48 h before being characterized by XRD.

2.3 Characterization

X-ray diffraction (XRD) patterns were recorded in a Shimadzu XRD-6000 diffractometer employing Cu Kα radiation (λ = 1.54056 Å) with Ni filter, 40 kV voltage and 30 mA current. The 2θ angle was scanned from 5° to 70° at a scanning rate of 2° min^{-1}. The diffraction lines were compared with XRD standards obtained from the Inorganic Crystal Structure Database (ICSD).

Scanning electron micrographs (SEM) were taken with an EVO® MA 10 microscope at accelerating voltages of 10 kV and 20 kV. Samples were placed in aluminum sample holders and covered by a thin layer of evaporated gold. Energy dispersive X-ray analysis (EDS) was performed using an Oxford instrument model 51-ADD0048.

Mass compositions were determined by Wavelength Dispersive X-Ray Fluorescence spectrometry (WDXRF) on a Bruker S8 Tiger equipment. Prior to characterization, samples were macerated and sieved in a 200-mesh sieve. The passing materials (which had a particle diameter size smaller than 74 µm) were used to produce pressed pellets. These pellets were made by mixing 1 g of the sample with 8 g of PXR 200 wax. Subsequently they were homogenized through maceration and pressed at 200 KPa.

The K recovery (the mass of extracted K divided by the mass of K in Verdete) was determined by flame photometry on an Analyzer 910MS equip-

ment. The extraction procedure was adapted from the methodology described by the Brazilian Ministry of Agriculture, Livestock and Supply (Brasil, 2014). In the adapted methodology, 0.5 g of sample is inserted into an Erlenmeyer flask with 100 mL of citric acid solution (20 g L^{-1}), then the mixture is stirred for 30 min and filtered with medium porosity filter paper. The filtrate is then diluted 5 times with distilled water and analyzed. The concentration of potassium (C_K, in ppm) obtained by flame photometry is converted into K recovery (R_K) with the following equation:

$$R_K \ (\%) \ = \ 100 \ \text{x} \left[\frac{\left(\dfrac{C_k}{1000000} \right) \text{x } 100 \text{ x } 5}{0.5 \ \text{x} \left(\dfrac{1}{1 + R_{R/V}} \right) \text{x } \dfrac{9.31}{100}} \right] \quad (1)$$

In Eq. (1), numbers 100, 5 and 0.5 refer respectively to the volume of citric acid solution, to the dilution factor and to the sample mass. The mass fraction of element K in Verdete is 9.31, which will be demonstrated later in the Results and Discussion – Characterization of Verdete section.

3. Results and discussion

3.1 Characterization of Verdete

Table 2 shows the mass fraction of elements (expressed as equivalent oxides) in five discrete size ranges of the three samples of Verdete. For better visualization, only those elements with mass fraction greater than 1% are displayed. The ore is composed mainly of SiO_2, Al_2O_3, K_2O, and other elements, such as Fe_2O_3 and MgO. These elements account for more than 95% of the sample masses. Comparatively, the K_2O contents are higher in samples collected from sites 1 and 3. The K_2O contents of particles passing the 200-mesh sieve are 11.28% (Sample 1) and 11.16% (Sample 3). Equal masses of these samples were then blended to generate a Verdete sample with 11.2 wt.% K_2O (or 9.31 wt.% K), which will be used in the next steps of this study.

Table 2 - Mass fraction of elements (expressed as equivalent oxides)in five discrete size ranges of the three samples of Verdete.

Sample	Size range	Mass fraction (%)				
		SiO_2	Al_2O_3	K_2O	Fe_2O_3	MgO
1	+35#	58.48	15.87	11.40	7.87	3.13
	+60#	59.32	16.51	11.45	8.00	3.15
	+100#	61.66	16.43	11.85	7.88	3.38
	+200#	59.89	16.32	11.46	7.66	3.18
	-200#	60.29	16.04	11.28	7.36	3.10
2	+35#	59.69	15.85	10.23	7.22	2.83
	+60#	62.80	16.22	10.60	7.55	3.04
	+100#	63.19	16.40	10.47	7.55	2.90
	+200#	62.34	15.90	10.46	7.39	2.95
	-200#	62.79	16.02	10.41	6.96	2.98
3	+35#	61.46	15.85	11.50	7.52	3.07
	+60#	61.91	15.80	11.41	7.60	3.11
	+100#	61.54	15.74	11.34	7.34	3.01
	+200#	61.18	15.70	11.41	7.49	3.06
	-200#	61.32	14.62	11.16	7.12	3.01

Fig. 1 shows the XRD pattern of the blended Verdete sample (+200-mesh sieve). Accordingly, the Verdete ore is composed of K-feldspar, micas (muscovite and glauconite) and quartz. The XRD pattern used to represent the K-feldspar group belongs to orthoclase (ICSD 10270). For a more in-depth discussion on possible types of K-feldspars that may be present in Verdete, please refer to the Supplemental Material. Orthoclase (KAlSiO$_3$) is a tectosilicate from K-feldspar group which has a continuous and negatively charged three-dimensional structure organized in SiO_4 and AlO_4 tetrahedra linked through their vertices (Lira and Neves, 2013). In Fig. 2, seven diffraction lines characteristic of K-feldspar (orthoclase) were identified (13.5°, 15.0°, 25.3°, 27.5°, 34.5°, 41.8° and 50.8°), which refer to the diffraction planes (0 2 0), (1 $\bar{1}$ 1), (1 $\bar{1}$ $\bar{2}$), (0 0 2), (3 $\bar{1}$ $\bar{2}$), (0 6 0) and (2 0 $\bar{4}$), respectively.
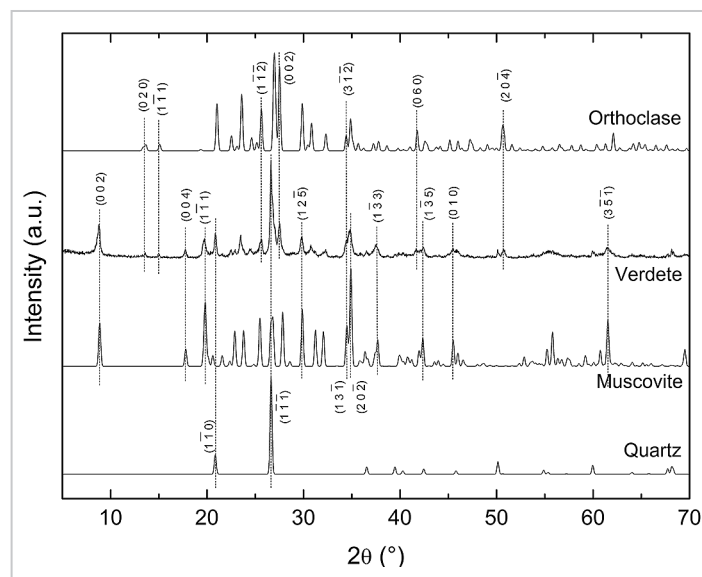
Figure 1 - XRD patterns of Verdete and references:
orthoclase (ICSD 10270), muscovite (ICSD 74608) and quartz (ICSD 174).

Muscovite is a phyllosilicate from the group of micas. Its atoms are in the maximum possible order required for space group C2/c, which generates a microscopic structure of very thin sheets, which grants softness and rupture in regular forms delimited by cleavage planes (perfect cleavage) (Radoslovich, 1960), as is observed in Verdete. The high-intensity diffraction lines identified at 8.5°, 17.8°, 20.0°, 29.8°, 35.0°, 37.0°, 42.2°, 45.5° and 61,7° correspond respectively to diffraction planes (0 0 2), (0 0 4), (1 $\bar{1}$ 0), (0 2 $\bar{5}$), (2 0 $\bar{2}$), (1 $\bar{3}$ 3), (1 $\bar{3}$ $\bar{3}$), (0 $\bar{1}$ 0) and (3 $\bar{5}$ $\bar{1}$) of muscovite (ICSD 74608). Diffraction lines at 21.8°, 24.8° and 29.0° of glauconite (ICSD 166961, not shown) do not have intense manifestation in the XRD pattern of Verdete. On the other hand, the compatibility of diffraction lines in several other angles, paired with similar macro-scopic characteristics, such as greenish color and softness (due to its laminar structural organization), indicates that glauconite is also a mineral of Verdete.

The presence of quartz (ICSD 174) in trigonal crystalline structure (SiO_2) should also be considered, due to the high amount of Si detected by XRF (Table 1) and to the high intensities of diffraction lines at 20.7° and 26.5° relative to diffraction planes (1 $\bar{1}$ 0) and (1 $\bar{1}$ $\bar{1}$) of the mineral.

3.2 Hydrothermal treatments

Fig. 2 shows the K recovery in series of reactions as a function of time. For detailed information on feeding conditions, please refer to Table 1. The low K recovery after reaction with water, $CaCl_2$ and $MgCl_2$ (Fig. 2a) indicates that these procedures were not effective in disrupting the crystalline structures of the minerals of Verdete. XRD patterns of the hydro-thermal products obtained after each of these reactions can be found in the Supplemental Material. Reactions with H_2SO_4 and $Ca(OH)_2$ are discussed in detail below.
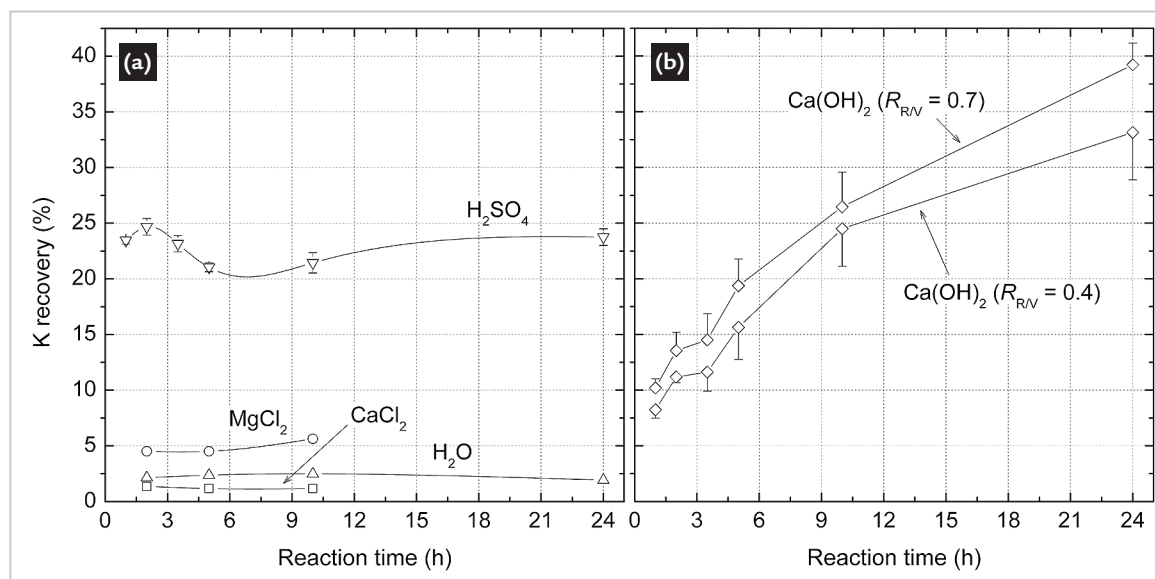

Figure 2 - Potassium recovery in series of reactions as a function of time.

3.3 Treatment of Verdete with H_2SO_4

Fig. 2a indicates that most of the reaction of Verdete with sulfuric acid occurs during the first hour. The K recovery in H_2SO_4 peaks at approximately 24% after 2 h of reaction time. The peak is then followed by a smooth decrease in K recovery until 5 h of reaction time, indicating that the reaction shifts to the formation of reactants between 2 and 5 h. After 10 h, K recovery increases again with time.

Fig. 3 displays the XRD patterns of hydrothermal products of the reaction with sulfuric acid as a function of time. These XRD patterns indicate that the micas (muscovite and glauconite, indicated by the letter µ), are no longer present after 1 h of reaction time, given that their respective diffraction lines are no longer observable in the diffractogram. The XRD patterns also indicate a probable crystallization of two distinct types of products. The first one likely being a combination of steklite $[KAl(SO_4)_2]$ and yavapaiite $[KFe(SO_4)_2]$, whose diffraction lines are indicated by Greek letter α. The second one, indicated by β, likely refers to an aluminum sulfate hydrate (or alum).
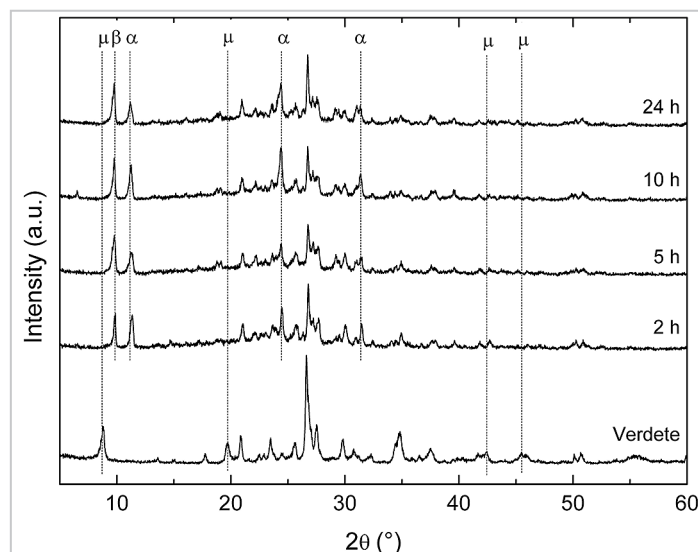

Figure 3 - XRD patterns of hydrothermal products of Verdete with H_2SO_4. Greek letters likely refer to diffraction lines of (α) steklite $[KAl(SO_4)_2]$ and yavapaiite $[KFe(SO_4)_2]$, (β) aluminum sulphate hydrate and (µ) micas.

In order to improve the identification of the formed or consumed structures, the hydrothermal product obtained after 10 h was filtered, and both fractions (filtered and retained) were characterized by XRD and EDS. The respective XRD patterns are shown in Figs. 4a (retained fraction) and 4b (filtered fraction). SEM micrographs are shown in Figs. 5a (retained fraction) and 5b (filtered fraction), and EDS results are presented in Table S2 (Supplementary Material).
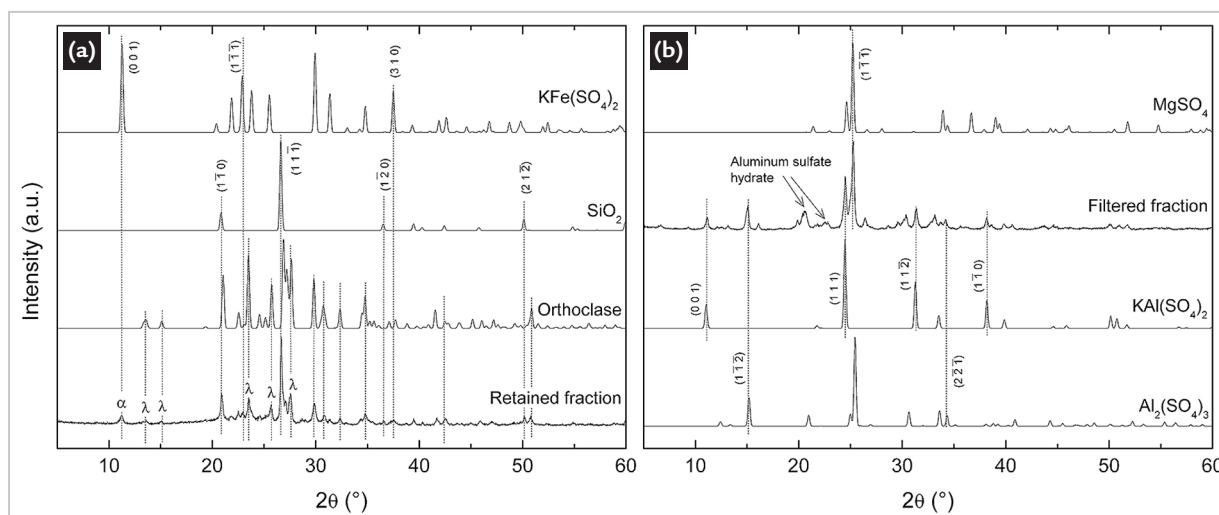

Figure 4 - XRD patterns of (a) retained and (b) filtered fractions of hydrothermal products of Verdete with H_2SO_4. Greek letters refer to diffraction lines of (α) yavapaiite $[KFe(SO_4)_2]$ and (λ) K-feldspar.

On the one hand, according to Fig. 4a, the retained fraction of the hydrothermal product obtained after 10 h reaction seems to consist of yavapaiite, K-feldspar and SiO_2. The latter being reminiscent of the initial composition of Verdete (see Fig. 1). Its triclinic structure is evidenced by diffraction lines at 21°, 26°, 36.5° and 50.5°, resulting from diffraction in planes ($1\bar{1}0$), ($1\bar{1}\bar{1}$), ($1\bar{2}0$) and ($21\bar{2}$), respectively. Diffraction lines identified by λ points to the presence of K-feldspar. This mineral is also reminiscent of the initial composition of Verdete, indicating that the reaction with sulfuric acid was not effective in disrupting its crystalline lattice as it did with micas, whose diffraction lines were not detected by XRD. Moreover, the

absence of Mg in the retained fraction, shown by EDS (Table S2 of Supplementary Material), confirms the complete destruction of the crystal structure of glauconite, the only mineral of Verdete bearing the element.
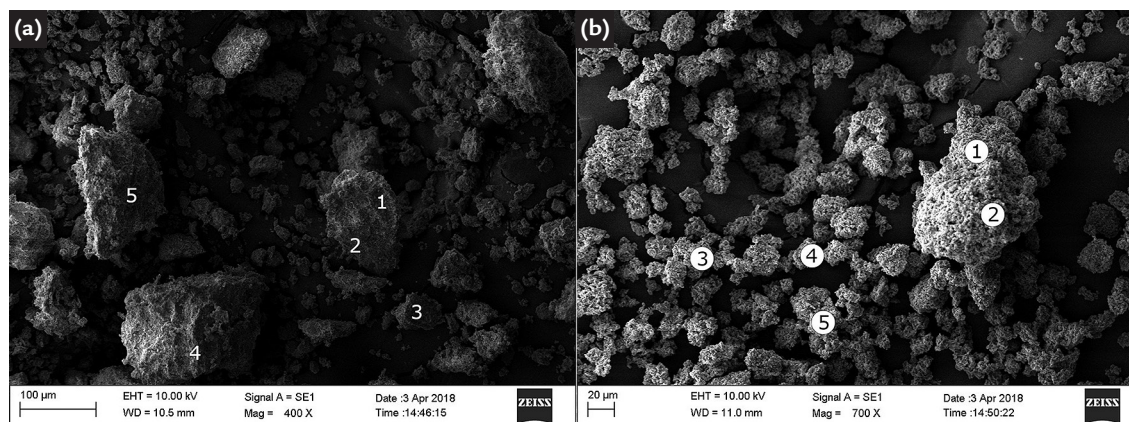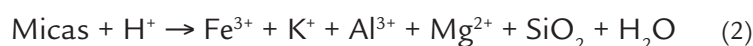

Figure 5 - SEM micrographs of (a) retained and (b) filtered fractions of the product obtained after 10 h reaction of Verdete with H_2SO_4. Refer to Table S2 (Supplementary Material) for the respective EDS results.

$$\text{Micas} + H^+ \rightarrow Fe^{3+} + K^+ + Al^{3+} + Mg^{2+} + SiO_2 + H_2O \qquad (2)$$

Once ionic exchange of H^+ with Fe^{3+}, K^+, Al^{3+} and Mg^{2+} occurred on the surface of muscovite and glauconite, the reaction mixture was composed of these ions coupled with SO_4^{2-} anions, generated from the dissociation of the sulfuric acid. Subsequently to filtration, the composition of hydrothermal products must obey crystallization equilibrium rules, which will not be discussed here. In Fig. 2, the existence of the point of maximum K recovery may be due to the decomposition of the crystalline structure of micas, which released K+, Fe^{3+}, Al^{3+} and Mg^{2+} into the reaction medium. It is worth noting that, in crystallized Fe-based compounds ($KFe(SO_4)_2$ and $Fe_2(SO_4)_3$), iron was under the Fe^{3+} form (ferric ion), which derived from the decomposition of glauconite.

3.4 Treatment of Verdete with $CaCO_3$ and $Ca(OH)_2$

Unlike the reactions performed with sulfuric acid, which reached maximum K recovery (approximately 24%) after 2 h, reactions with calcined $CaCO_3$ presented a gradual increase of K recovery over the 24 h reaction period (see Fig. 2). It is also noted that increasing the $R_{R/V}$ ratio from 0.4 to 0.7 leads to increased K recovery.

XRD patterns of the hydrothermal products obtained from the reaction of Verdete with calcined $CaCO_3$ ($R_{R/V} = 0.6$) are shown in Fig. 6. The diffraction lines of micas, represented by Greek letter μ, did not lose intensity over time, which indicates that muscovite and glauconite were not consumed during the treatment. Regarding the three diffraction lines belonging to $CaCO_3$ (identified by γ), it was noted that, between 5 h and 10 h, the K recovery increased from 19.7% to 26.8%. However, those lines did not lose intensity, suggesting that there was little to no consumption of $CaCO_3$ throughout the treatment. The diffraction lines identified by λ, related to K-feldspar, and π, related to $Ca(OH)_2$, lost intensity significantly over the reaction period, which suggests that both substances were consumed during the process.
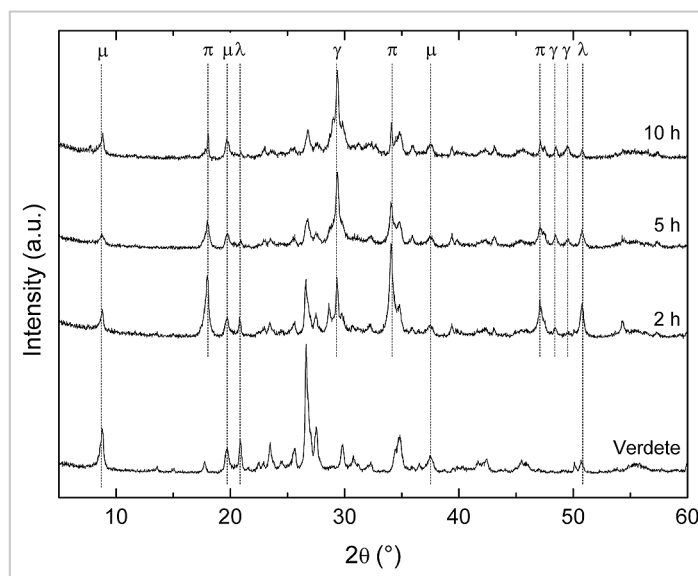

Figure 6 - XRD patterns of hydrothermal products of Verdete with calcined $CaCO_3$. Greek letters refer to diffraction lines of (γ) $CaCO_3$, (μ) micas, (ϖ) $Ca(OH)_2$ and (λ) K-feldspar.

For better identification of formed and consumed phases, the hydrothermal products obtained after 10 h were filtered and both fractions (filtered and retained) were characterized by XRD and EDS. The respective XRD patterns are shown in Figs. 7a (retained fraction) and 7b (filtered fraction). SEM micrographs are shown in Figs. 8a (retained fraction) and 8B (filtered fraction), and EDS results are presented in Table S3 (Supplementary Material).

Fig. 7a shows that the retained fraction is composed of $CaCO_3$, $Ca(OH)_2$ and all the minerals from Verdete (micas, K-feldspar and SiO_2). EDS results confirm the presence of O, Ca, Si, C, K, Al, Fe and Mg (Table S3 of Supplementary Material). Similar to the XRD patterns previously presented in Fig. 6, the diffraction lines of micas (represented by μ) did not lose intensity, indicating that the muscovite and glauconite were not consumed during the process. Nonetheless, the XRD pattern of the filtered fraction (Fig. 7b) presents diffraction lines characteristic of $CaCO_3$ (represented by γ) and $K_2Ca(CO_3)_2$ (represented by ε). Popularly known as bütschliite, the latter compound is recognized by diffraction lines at 31°, 33.5°, 39.8° and 44°, relative to planes $(1\,\bar{1}\,5)$, $(1\,\bar{1}\,0)$, $(2\,\bar{2}\,\bar{2})$ and $(2\,0\,\bar{4})$, respectively. It is important to note that the filtered fraction shows no evidence of $Ca(OH)_2$, or any other alkali. EDS results (Table S3 from Supplementary Material) also corroborate with the XRD pattern from Fig. 7a, since the elements detected in the five points (O, Ca, C and K) are those necessary for $CaCO_3$ and $K_2Ca(CO_3)_2$ formation. Specifically in points 2 and 3, the presence of elongated crystals is notable.
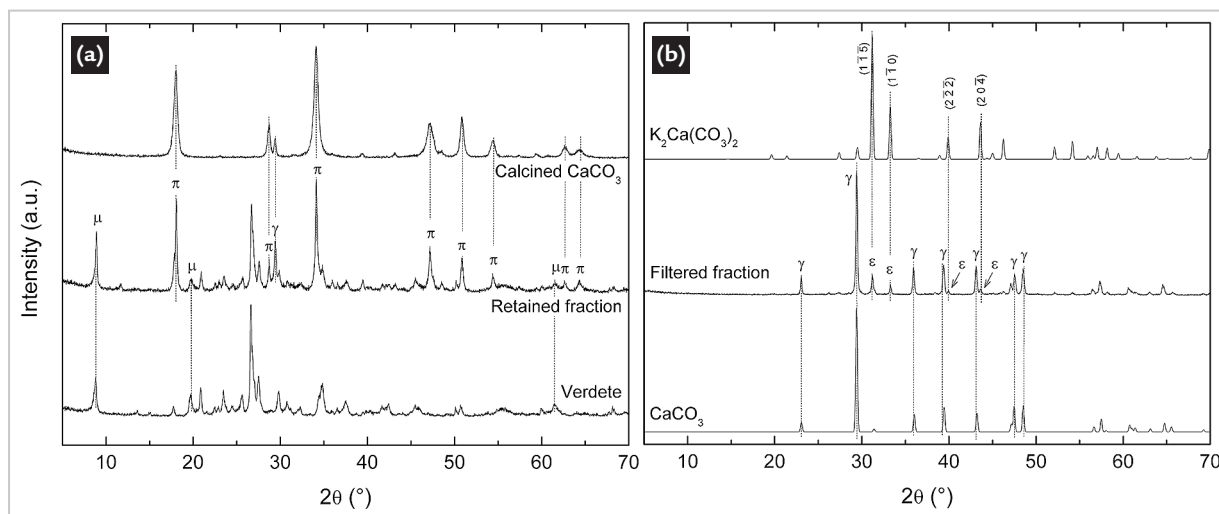

Figure 7 - XRD patterns of (a) retained and (b) filtered fractions of products of Verdete with calcined $CaCO_3$. Greek letters refer to diffraction lines of (γ) $CaCO_3$, (μ) micas, (ϖ) $Ca(OH)_2$ and (ε) bütschliite [$K_2Ca(CO_3)_2$].
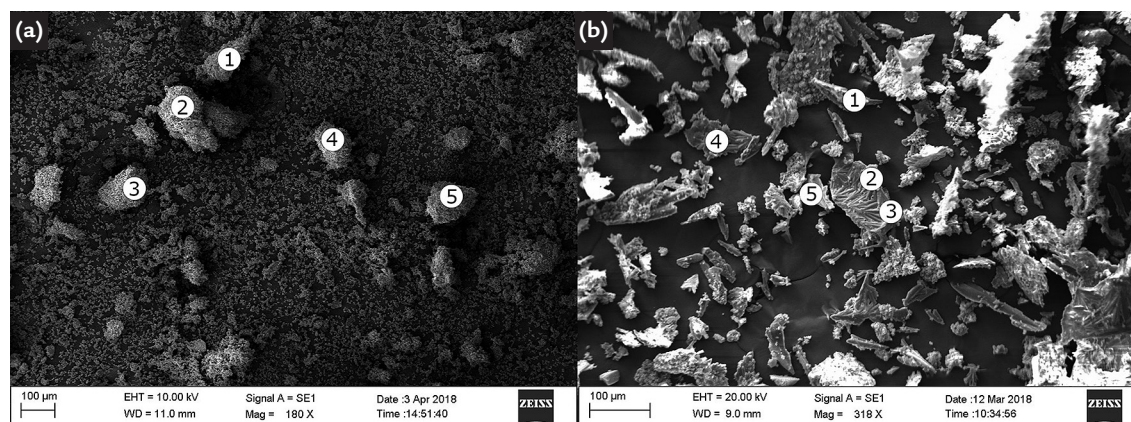

Figure 8 - SEM micrographs of (a) retained and (b) filtered fractions of the product obtained after 10 h reaction of Verdete with calcined $CaCO_3$. Refer to Table S3 (Supplementary Material) for the respective EDS results.

The aforementioned micas did not appear to evidence its decomposition over the treatment with calcined $CaCO_3$ (14% $CaCO_3$ and 86% $Ca(OH)_2$ in mass). In addition to the non-disappearance of the diffraction lines related to micas (see Figs. 6 and 7a), the EDS results (Table S3 of Supplementary Material) indicated that iron, which could only be found in glauconite, was not present as a decomposition product in the filtered fraction. Consequently, the K recovery curve shown in Fig. 2 derived from the decomposition of K-feldspar over time. Unlike the treatment with sulfuric acid, in which the micas were decomposed releasing K^+, Fe^{3+}, Al^{3+} and Mg^{2+}, the decomposition process of K-feldspar was gradual with time. It was not possible to observe structural changes of K-feldspar through XRD analysis, but it is likely that the mechanism of K^+ release was due to a concurrent hydrolytic dissolution framework mediated by OH^- ions and by the exchange of K+ for Ca^{2+}, as proposed by Ciceri *et al.* (2017). As shown in Fig. 7b, despite the complexity of the hydrothermal product, it is likely that the K-bearing species are carbonaceous materials with variable K^+/Ca^{2+} ratios, such as $K_2Ca(CO_3)_2$.

4. Conclusions

The Verdete rock, collected in the central region of Minas Gerais state (Brazil), is composed mostly of micas (glauconite and muscovite) and tectosilicates (K-feldspar and quartz), containing an equivalent K_2O content of 11.2% (in mass). The rock underwent hydrothermal treatment in stainless steel autoclaves internally coated with Teflon at 483 K in the presence of several reactants. $MgCl_2$- and $CaCl_2$ based treatments were not sufficient to break the crystal lattice of its respective minerals. In the presence of H_2SO_4 (5 mol L^{-1}), crystal lattices of glauconite and muscovite were dismantled in less than 1 h, leaching up to 24% of K in the form of sulfates. Leaching must have occurred through an ionic exchange mechanism of H^+ for Fe^{3+}, K^+, Al^{3+} or Mg^{2+} on the surface of micas. The crystalline structure of K-feldspar appears to have remained intact during the process, indicating the inefficiency of H_2SO_4 in breaking down its mineral structure. On the other hand, thermal treatment of Verdete with a $Ca(OH)_2$ (86 wt.%) - $CaCO_3$ (14 wt.%) mixture generated different results. In this case, the two micas were not consumed, and K recovery was probably due to a concurrent hydrolytic dissolution framework of K-feldspar mediated by OH^- ions and by K^+ for Ca^{2+} exchange. Furthermore, the K-bearing species are carbonaceous materials with variable K^+ to Ca^{2+} ratios, such as $K_2Ca(CO_3)_2$, and not potassium alkalis.

Acknowledgement

References

BRASIL. Ministério da Agricultura, Pecuária e Abastecimento. *Manual de métodos analíticos oficiais para fertilizantes minerais, orgânicos, organominerais e corretivos.* Brasília: MAPA/SDA/CGAL, 2014. 220 p.

CICERI, D.; OLIVEIRA, M.; ALLANORE, A. Potassium fertilizer via hydrothermal alteration of K-feldspar ore. *Green Chemistry,* v. 19, n. 21, p. 5187-5202, 2017.

CUSHMAN, A. S.; HUBBARD, P. The extraction of potash from feldspathic rock. *Journal of the American Chemical Society,* v. 30, n. 5, p. 779-797, 1908.

FOOTE, H. W.; SCHOLES, S. R. The extraction of potash and alumina from feldspar. *Journal of Industrial & Engineering Chemistry,* v. 4, n. 5, p. 377-377, 1912.

LIRA, H. L.; NEVES, G. A. Feldspatos: conceitos, estrutura cristalina, propriedades físicas, origem e ocorrências, aplicações, reservas e produção. *Revista Eletrônica de Materiais e Processos,* v. 8, n. 3, p. 110-117, 2013.

MARTINS, E. D. S.; OLIVEIRA, C. G. D.; RESENDE, A. V. D.; MATOS, M. S. F. D. Agrominerais: rochas silicáticas como fontes minerais alternativas de potássio para a agricultura In: ROCHAS e minerais industriais: usos e especificações. 2. ed. Rio de Janeiro: CETEM/MCT, 2008. p. 205-221.

MACKENZIE, W. S. The orthoclase-microcline inversion. *Mineralogical Magazine and Journal of the Mineralogical Society,* v. 30, n. 225, p. 354-366, 1954.

MOREIRA, D. S.; UHLEIN, A.; FERNANDES, M. L. S.; MIZUSAKI, A. M.; GALÉRY, R.; DELBEM, I. D. Estratigrafia, petrografia e mineralização de potássio em siltitos verdes do grupo Bambuí na região de São Gotardo, Minas Gerais. *Geociências,* v. 35, n. 2, p. 157-171, 2016.

PIZA, P. A. T.; BERTOLINO, L. C.; SILVA, A. A. S.; SAMPAIO, J. A.; LUZ, A. B. Verdete da região de Cedro de Abaeté (MG) como fonte alternativa para potássio. *Geociências,* v. 30, n. 3, p. 345-356, 2011.

RADOSLOVICH, E. The structure of muscovite, $KAl_2(Si_3Al)O_{10}(OH)_2$. *Acta Crystallographica,* v. 13, n. 11, p. 919-932, 1960.

SANTOS, W. O.; MATTIELLO, E. M.; VERGUTZ, L.; COSTA, R. F. Production and evaluation of potassium fertilizers from silicate rock. *Journal of Plant Nutrition and Soil Science,* v. 179, n. 4, p. 547-556, 2016.

SOARES, B. D. *Estudo da produção de óxido de cálcio por calcinação do calcário:* caracterização dos sólidos, decomposição térmica e otimização paramétrica. 2007. 422 f. Dissertação (Mestrado em Engenharia Química) – Faculdade de Engenharia Química, Universidade federal de Uberlândia, Uberlândia, 2007.

U.S. GEOLOGICAL SURVEY. *Mineral commodity summaries 2018.* Reston, VA: U.S. G. S., 2018. 200 p.

TEIXEIRA, A. M. S.; SAMPAIO, J. A.; GARRIDO, F. M. S.; MEDEIROS, M. E. Avaliação da rocha fonolito como fertilizante alternativo de potássio. *Holos,* v. 5, p. 21-33, 2012.

VARADACHARI, C. An investigation on the reaction of phosphoric acid with mica at elevated temperatures. *Industrial & Engineering Chemistry Research,* v. 31, n. 1, p. 357-364, 1992.

VARADACHARI, C. Potash fertilizer from biotite. *Industrial & Engineering Chemistry Research,* v. 36, n. 11, p. 4768-4773, 1997.

WANG, Z.; ZHANG, Q.; YAO, Y.; JIA, Y.; XIE, B. The extraction of potassium from K-feldspar ore by low temperature molten salt method. *Chinese Journal of Chemical Engineering,* v. 26, n. 4, p. 845-851, 2018.

Supplementary material

Calcination of $CaCO_3$

Calcination of calcium carbonate ($CaCO_3$) is widely applied to obtain calcium oxide (CaO), commonly known as quicklime, which also releases carbon dioxide (Reaction S1).

$$CaCO_{3(S)} \rightarrow CaO_{(S)} + CO_{2(G)} \qquad \text{(Reaction S1)}$$

Quicklime is a white powder with several applications, mainly in the construction industry, where it is used to prepare mortar. Its large-scale production is usually carried out in rotary kilns at 1173 K, obtaining conversion of about 90%. In laboratory scale, it is possible to achieve similar conversion in muffle furnace at 1173 K and 30 min [1]. Based on this information, calcium carbonate (Cinética Química, 99%) was distributed in seven porcelain crucibles (with the purpose of increasing surface area) and calcined in muffle furnace at 1173 K for 30 min under flow of atmospheric air. Initial masses of $CaCO_3$ and final masses of calcined products are shown in Table S1.

Table S1 - Results of the $CaCO_3$ calcination procedure.

Crucible number	Mass of $CaCO_3$ before calcination (g)	Mass after calcination (g)
1	7.19	5.49
2	7.19	5.48
3	7.18	5.51
4	7.22	5.54
5	7.12	5.44
6	7.21	5.61
Sum	43.11	33.07

After calcination, the seven products were mixed and the blend was characterized by XRD (Fig. S1). The XRD pattern of this blend is composed of $CaCO_3$ and $Ca(OH)_2$ diffraction lines. This indicates that, in addition to the residual presence of unreacted $CaCO_3$, formation of $Ca(OH)_2$ occurred from hydration of CaO (Reaction S2) with air humidity inside the muffle furnace during calcination.

$$CaO_{(S)} + H_2O_{(V)} \rightarrow Ca(OH)_{2(S)} \qquad \text{(Reaction S2)}$$
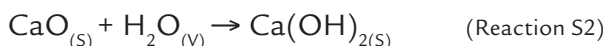
In view of these results, composition of the calcination product can be estimated as follows:

$$M_F = M_{CaCO_3} + M_{Ca(OH)_2} = 100 \times (N_{CaCO_3,\,0} - \xi_{S1}) + 74\,\xi_{S2}$$
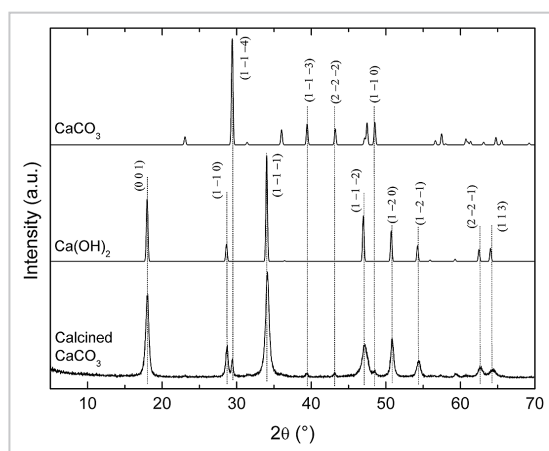

Fig. S1 - XRD pattern of the blend of $CaCO_3$ calcination products. XRD patterns of $Ca(OH)_2$ and $CaCO_3$ were obtained in the Inorganic Crystal Structure Database (ICSD) [collection codes 202228 and 190275, respectively].

Since XRD lines of CaO were not observed in Fig. S1, it will be assumed that the whole product was consumed by reaction S2, i.e., $\xi_{S2} = \xi_{S1}$. Thus,

$$M_F = M_{CaCO_3} + M_{Ca(OH)_2} = 100 \times (N_{CaCO_3,\,0} - \xi_{S1}) + 74\,\xi_{S1}$$

$$\xi_{S1} = (100 N_{CaCO_3,\,0} - M_F)/26$$

In the previous deduction, variables are defined as: M_F = total mass after calcination, M_{CaCO_3} = total mass of unreacted $CaCO_3$, $M_{Ca(OH)_2}$ = total mass of $Ca(OH)_2$ formed after calcination, $N_{CaCO_3,0}$ = total number of mols of $CaCO_3$ before calcination, ξ_{S1} = extent of Reaction S1, ξ_{S2} = extent of Reaction S2.
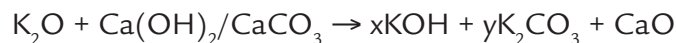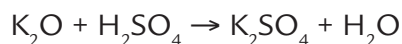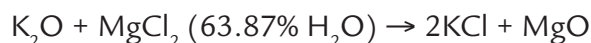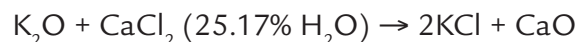
Since M_F = 33.07 g and $N_{CaCO_3,0}$ = 0.4311 mol, then ξ_{S1} = 0.3861 mol, M_{CaCO_3} = 4.49 g and $M_{Ca(OH)_2}$ = 28.57 g. Thus, the blend of $CaCO_3$ calcination products is composed of 14% $CaCO_3$ and 86% $Ca(OH)_2$ (in mass).

Estimating reactor feed conditions

For calculation purposes, we have considered the Verdete to be pure K_2O. Although the K_2O content in the ore is much lower (~11%), the above consideration was used to consider possible consumption of reactants in parallel reactions. Thus, we have proposed the following model reactions to estimate the reactant masses:

$$K_2O + CaCl_2 \ (25.17\% \ H_2O) \rightarrow 2KCl + CaO$$

$$K_2O + MgCl_2 \ (63.87\% \ H_2O) \rightarrow 2KCl + MgO$$

$$K_2O + H_2SO_4 \rightarrow K_2SO_4 + H_2O$$

$$K_2O + Ca(OH)_2/CaCO_3 \rightarrow xKOH + yK_2CO_3 + CaO$$

The reactant masses were calculated to respect the stoichiometry of such reactions, which generated the values of $R_{W/V}$ and $R_{R/V}$.

Possible types of K-feldspar in Verdete

In this work, the XRD pattern used to represent the K-feldspar group belongs to orthoclase. However, the K-feldspar group consists of four minerals: orthoclase, sanidine, microcline and anorthoclase. Fig. S2 shows the XRD patterns of Verdete and these structures.
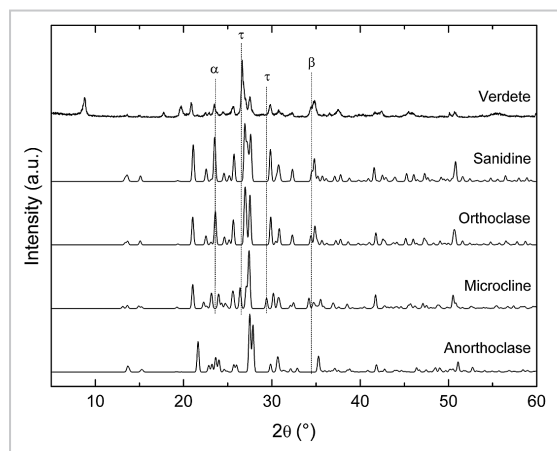

Fig. S2 - XRD patterns of Verdete and references of K-feldspar minerals: orthoclase (ICSD 10270), sanidine (ICSD 9583), microcline (ICSD 35335) and anorthoclase (ICSD 34742).

Sanidine is the monoclinic polymorphic mineral of orthoclase. Its stability at high temperatures, due to the typical formation in this condition and subsequent rapid cooling, reflects its disordered structure based on Al and Si tetrahedral [2]. The XRD patterns of sanidine and orthoclase are very similar and, thus, either of the two minerals may be the K-feldspar of Verdete, or even both can coexist.

The diffraction lines of orthoclase and microcline, in turn, present larger differences, the most evident ones being identified by symbols α and τ. The diffraction peak identified by α at 23.5°, which corresponds to orthoclase plane (0 1 $\overline{2}$) is not present in microcline; while at 26.5° and 29.5°, symbol τ identifies two diffraction peaks of microline that are not present in orthoclase. In spite of these differences, the coexistence of both structures in Verdete should be considered, mainly due to the strong similarity between the rest of the diffraction lines and the possible metamorphism between monoclinic (orthoclase) and triclinic (microcline) symmetry [3].

The XRD pattern of anorthoclase is also very similar to that of orthoclase, except for diffraction line at 34.5°, which refers to plane (3 $\overline{1}$ $\overline{2}$) of orthoclase, indicated by β. The XRD pattern of Verdete has a peak at this position, but it may also originate from diffraction of muscovite plane (1 3 $\overline{1}$) (as shown in Fig. 2). Thus, anorthoclase may be considered a possible K-feldspar of Verdete.

Reaction of Verdete with water

Fig. S3 shows the XRD patterns of products obtained after reaction of Verdete with pure water.
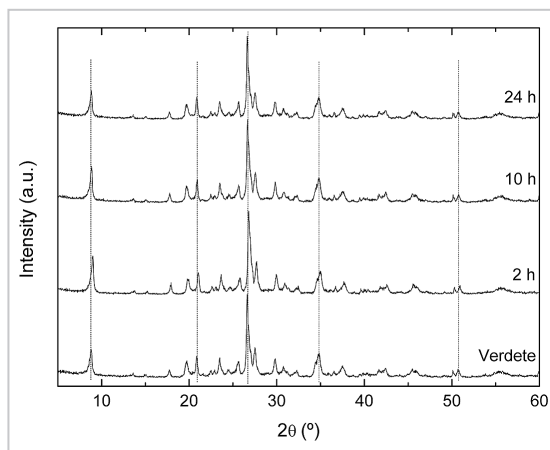

Fig. S3 - XRD patterns of products obtained after reaction of Verdete with water at various reaction times.

Reaction of Verdete with CaCl$_2$

Fig. S4 shows the XRD patterns of products obtained after reaction of Verdete with $CaCl_2$. After 2 and 5 h of reaction, the XRD patterns indicate

the presence of Verdete minerals and $CaCl_2 \cdot xH_2O$, where x may be 2, 4 and 6. After 10 h, hydration increases, leaving mostly $CaCl_2 \cdot 6H_2O$.
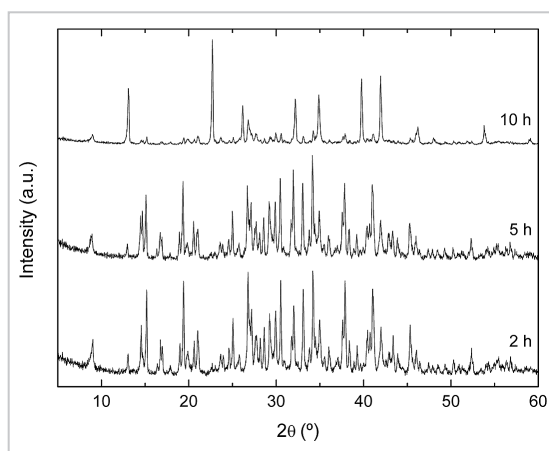

Fig. S4 - XRD patterns of products obtained after reaction of Verdete with $CaCl_2$ at various reaction times.

Reaction of Verdete with $MgCl_2$

Fig. S5 shows the XRD patterns of products obtained after reaction of Verdete with $MgCl_2$. XRD patterns obtained after 2 and 5 h indicate the presence of Verdete minerals and $MgCl_2 \cdot 6H_2O$. The intensity of diffraction lines characteristic of $MgCl_2 \cdot 6H_2O$ decreases significantly after 10 h of reaction.
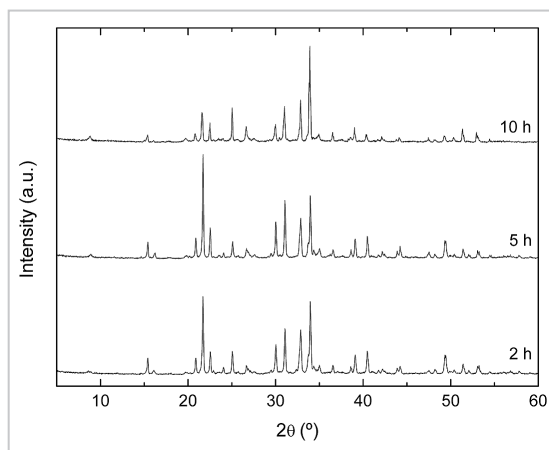

Fig. S5 - XRD patterns of products obtained after reaction of Verdete with $MgCl_2$ at various reaction times.

EDS

Table S2 - EDS results of retained and filtered fractions of the hydrothermal product obtained after 10 h reaction of Verdete with H_2SO_4. Refer to Fig. 5 to visualize the points at which the X-ray beam was focused.

Fraction	Point	O (%)	Si (%)	Al (%)	K (%)	Fe (%)	Mg (%)	S (%)
Retained	1	44.8	23.4	1.7	4.1	2.1	-	3.9
	2	40.7	23.4	2.9	3.5	0.6	-	-
	3	33.6	26.8	2.1	4.7	1.5	-	-
	4	29.8	26.0	2.3	5.0	1.6	-	-
	5	36.8	22.2	2.9	6.9	3.7	-	-
Filtered	1	49.6	-	5.6	1.5	1.0	1.9	18.2
	2	40.1	-	3.8	2.7	2.5	0.8	20.7
	3	46.9	-	5.9	4.8	1.0	1.6	20.5
	4	40.7	-	6.3	1.2	0.7	2.2	13.2
	5	46.8	-	6.5	3.0	3.0	1.3	30.9

* The remaining percentage consists of gold and other elements less expressive of Verdete.

Table S3 - EDS results of retained and filtered fractions of the hydrothermal product obtained after 10 h reaction of Verdete with calcined CaCO₃. Refer to Fig. 8 to visualize the points at which the X-ray beam was focused.

Fraction	Point	O (%)	Ca (%)	Si (%)	C (%)	Al (%)	K (%)	Fe (%)	Mg (%)
Retained	1	32.7	21.6	9.1	6.3	2.3	3.4	2.0	0.6
	2	43.0	24.1	3.8	6.3	1.3	0.9	0.7	0.3
	3	34.2	24.5	5.6	6.1	1.1	1.1	0.7	0.3
	4	37.6	12.1	9.8	6.7	3.4	3.2	1.7	0.8
	5	32.4	29.5	5.7	5.2	1.4	2.1	1.4	0.4
Filtered	1	35.2	29.6	-	10.7	-	3.3	-	-
	2	34.4	22.7	-	12.9	-	2.5	-	-
	3	22.1	16.2	-	8.8	-	21.3	-	-
	4	30.2	24.9	-	8.8	-	1.1	-	-
	5	18.9	29.8	-	6.1	-	1.8	-	-

* The remaining percentage consists of gold and other elements less expressive of Verdete.